2022-02-01

In vitro toxicological evaluation of mesoporous silica microparticles functionalised 1 with carvacrol and thymol

Cristina Fuentes
Universidad Politecnica de Valencia, crifuelp@upvnet.upv.es

Ana Fuentes
Universidad Politecnica de Valencia

Hugh Byrne
Technological University Dublin, hugh.byrne@tudublin.ie

See next page for additional authors

Recommended Citation

Cristina Fuentes, Ana Fuentes, Hugh J. Byrne, José Manuel Barat, María José Ruiz, In vitro toxicological evaluation of mesoporous silica microparticles functionalised with carvacrol and thymol, Food and Chemical Toxicology, Volume 160, 2022, 112778, ISSN 0278-6915, DOI: 10.1016/j.fct.2021.112778.

Funder: Government of Spain

In vitro toxicological evaluation of mesoporous silica microparticles functionalised with carvacrol and thymol

Cristina Fuentes[a1], Ana Fuentes[a], Hugh J. Byrne[b], José Manuel Barat[a], María José Ruiz[c]

[a]Department of Food Technology, Universitat Politècnica de València. Camino de Vera s/n, 46022, València, Spain

[b]FOCAS Research Institute, City Campus, Technological University Dublin, Dublin 8, Ireland

[c]Laboratory of Toxicology, Faculty of Pharmacy, Universitat de València, Av. Vicent Andrés Estellés s/n, 46100 Burjassot, València, Spain

[1]**Corresponding author** Cristina Fuentes. Department of Food Technology, Universitat Politècnica de València. Camino de Vera s/n, 46022, Valencia, Spain: crifuelp@upvnet.upv.es

Abbreviations

ΔΨm, Mitochondrial membrane potential; APTES, (3-aminopropyl)triethoxysilane; BHT, di-ter-butyl- methylphenol; CTAB, Hexadecyltrimethylammonium bromide; DFA, Deferoxamine mesylate salt; DMEM, Dulbecco's Modified Eagle Medium; DMSO, Dimethyl sulfoxide; EOCs, essential oil components; H_2-DCFDA, 2′,7′-dichlorodihydrofluorescein diacetate, IC_{50}, Mean inhibition concentration; LDH, Lactate dehydrogenase; LPO, lipid peroxidation; MCM-41, Mobile crystalline material-41; MDA, Malondialdehyde; MTT, thiazolyl blue tetrazolium bromide; NBCS, Newborn calf serum; PBS, phosphate buffered saline; PI, Propidium Iodide; ROS, Reactive oxygen species; TBA, thiobarbituric acid; TBARS, Thiobarbituric acid reactive substances; $TEAH_3$, Triethanolamine; TEM, Transmission electron microscopy

Abstract

The cytotoxicity of carvacrol- and thymol- functionalised mesoporous silica microparticles (MCM-41) was assessed in the human hepatocarcinoma cell line (HepG2). Cell viability, lactate dehydrogenase (LDH) activity, reactive oxygen species (ROS) production, mitochondrial membrane potential (ΔΨm), lipid peroxidation (LPO) and apoptosis/necrosis analysis were used as endpoints. Results showed that both materials induced cytotoxicity in a time and concentration-dependent manner, being more cytotoxic than free essential oil components and bare MCM-41. This effect was caused by the cell-particle interactions and not from degradation products released to the culture media, as demonstrated in the extract dilution assays. LDH release was seen to be a less sensitive endpoint than the MTT (thiazolyl blue tetrazolium bromide) assay, suggesting impairment of the mitochondrial function as the primary cytotoxic mechanism. *In vitro* tests on specialised cell functions showed that exposure to sublethal concentrations of these materials did not induce ROS formation within 2-h exposure but produced LPO and ΔΨm alteration in a concentration-dependent manner when cells were exposed for 24 h. Overall, the results found in this study support the hypothesis that carvacrol- and thymol-functionalised MCM-41 microparticles induced toxicity in HepG2 cells by an oxidative stress-related mechanism that resulted in apoptosis through the mitochondrial pathway.

Keywords: mesoporous microparticles; silica; essential oil components; cytotoxicity; HepG2

1. Introduction

Consumer awareness of additives and chemicals in their diets has forced the food industry to search for alternatives to synthetic preservatives to extend the shelf life of their products (Faleiro and Miguel, 2020; Ribes et al., 2018). In this regard, essential oils and their constituent components have attracted considerable attention, due to their natural origin and their well-known antimicrobial and antioxidant activity (Burt, 2004; Hyldgaard et al., 2012). The monoterpenoids carvacrol and thymol, major components in essential oils from different plant species such as origanum or thyme, are two of the most investigated essential oil components (EOCs), due to their strong action against a wide spectrum of foodborne and food spoilage microorganisms (Abbaszadeh et al., 2014; Abdelhamid and Yousef, 2021; Čabarkapa et al., 2019; Karam et al., 2019; Tippayatum and Chonhenchob, 2007; Walczak et al., 2021). The antimicrobial action of these components has been mainly attributed to the presence of a hydroxyl group and a system of delocalised electrons in their chemical structure, able to disrupt the cytoplasmic membrane, leading to leakage of intracellular content and ultimately lysis (Xu et al., 2008). However, their application in food products presents some challenges, such as high volatility, low solubility or strong sensory properties (Hyldgaard et al., 2012). In this regard, grafting of EOCs onto the surface of silica particles has been proposed as a strategy to increase the antimicrobial activity of these components and to overcome their drawbacks. These hybrid organic-inorganic particles have efficiently performed as preservatives in different food matrices (Ribes et al., 2019, 2017) and as filtering materials for the cold pasteurisation of beverages (García-Ríos et al., 2018; Peña-Gómez et al., 2020, 2019b, 2019a).

Among mesoporous silica materials, Mobil Composition of Matter (MCM)-41 is one of the most widely employed scaffolds for the synthesis of organic-inorganic hybrid

systems, due to the ease of surface functionalisation, large surface area, uniform pore size and high stability (Diab et al., 2017). Moreover, as a result of the high biocompatibility and low toxicity reported (Aburawi et al., 2012; Al-Salam et al., 2011; Garrido-Cano et al., 2021), MCM-41 materials have been studied for the covalent attachment of functional groups and organic molecules in a number of oral applications (Bagheri et al., 2018; Ros-Lis et al., 2018). However, as the surface properties of particles are key factors for determining their interactions with biological systems (Kyriakidou et al., 2020; Puerari et al., 2019; Vicentini et al., 2017), the analysis of the *in vitro* and *in vivo* behaviour of surface modified silica structures is crucial to guarantee the safety and innocuousness of their use for human health.

Previous *in vitro* studies have evaluated the stability of different types of synthetic amorphous silica particles functionalised with carvacrol, eugenol and vanillin under conditions that represented the human gastrointestinal tract and lysosomal fluid (Fuentes et al., 2021, 2020). Results showed that functionalisation with these EOCs resulted in lower dissolution levels than bare MCM-41 microparticles, and therefore increased stability under both biological conditions (Fuentes et al., 2020). Conversely, the comparative analysis of the cytotoxic effect of eugenol and vanillin functionalised silica particles revealed that free EOCs and bare particles had a milder cytotoxic effect on HepG2 cells than functionalised MCM-41 materials. A relationship between cytotoxicity and the density of EOC molecules on the surface of the functionalised particles was found. According to the physico-chemical analysis of the materials, properties such as cationic nature and hydrophobicity were suggested to enhance the cytotoxic behaviour of the functionalised silica particles (Fuentes et al., 2021). All together, these results demonstrate that functionalisation of MCM-41 particles with EOCs derivatives enhances the stability of these materials under biological conditions, but may increase their

cytotoxic behaviour, leading to potential toxicological hazards. However, the molecular mechanism underlying the cytotoxic behaviour of these materials remains to be elucidated. Accordingly, in this work we aimed to investigate the cytotoxic effect of carvacrol and thymol functionalised MCM-41 microparticles and further to elucidate the related toxicity mechanism. To this end, HepG2 human liver cells were exposed to the modified silica materials and cell viability, lactate dehydrogenase (LDH) activity, reactive oxygen species (ROS) production, mitochondrial membrane potential ($\Delta\Psi m$), lipid peroxidation (LPO) and apoptotic and necrotic responses were evaluated.

2. Materials and methods

2.1. Reagents

Triethanolamine ($TEAH_3$), hexadecyltrimethylammonium bromide (CTAB), carvacrol (≥ 98% w/w), thymol (≥ 99% w/w), (3-aminopropyl) triethoxysilane (APTES), thiazolyl blue tetrazolium bromide (MTT), 2′,7′-di- chlorodihydrofluorescein diacetate (H2-DCFDA), Rhodamine 123, thiobarbituric acid (TBA), deferoxamine mesylate salt (DFA) and di-ter-butyl- methylphenol (BHT) were obtained from Sigma-Aldrich (Spain). Dimethyl sulfoxide (DMSO) was purchased from Scharlab (Spain).

The HepG2 human hepatocarcinoma cell line was obtained from the American Type Culture collection (ATCC HB-8065). Dulbecco's Modified Eagle Medium (DMEM-Glutamax™) with high glucose (4.5 g/L), phosphate buffered saline (PBS), newborn calf serum (NBCS), penicillin, streptomycin, trypsin-EDTA 0.5% and sodium pyruvate were supplied by Gibco (Life- Technologies, USA).

2.2. Preparation of EOCs-functionalised MCM-41 microparticles

The mesoporous silica microparticles MCM-41 were prepared through the 'atrane route', which is based on the use, under basic conditions, of $TEAH_3$, that generates atrane

complexes as inorganic hydrolytic precursors and CTAB as structural directing agent (Cabrera et al., 2000). The procedure of the synthetic process is fully described at (Fuentes et al., 2020).

Once synthesised, the functionalisation of the MCM-41 silica particles with carvacrol and thymol was performed by a three-stage protocol that includes: (1) synthesis of carvacrol and thymol aldehyde derivatives by direct formylation with paraformaldehyde; (2) synthesis of alkoxysilane derivatives by reaction of carvacrol and thymol aldehydes with APTES; and (3) immobilisation of the alkoxysilane derivatives on the surface of silica particles (García-Ríos et al., 2018).

2.3. Physico-chemical characterisation of MCM-41 microparticles

Bare and functionalised MCM-41 microparticles were analysed by transmission electron microscopy (TEM), particle size distribution, zeta potential and elemental analysis. For the morphological analysis of the materials by TEM, particles were dispersed in dichloromethane and sonicated for 2 min to avoid aggregation. The suspension was placed onto copper grids coated with carbon film (Aname SL, Spain). Imaging of the particle samples was done using a JEOL JEM-1010 (JEOL Europe SAS, France), operating at an acceleration voltage of 80 kV. The zeta potential of the particles was studied by laser Doppler microelectrophoresis using a Zetasizer Nano ZS (Malvern Instruments, UK) and the Smoluchowski mathematical model. Particle size distribution was determined using a laser diffractometer (Mastersizer 2000, Malvern Instruments, UK) and application of Mie theory (refractive index of 1.45, absorption index of 0.1). For both zeta potential and particle size distribution analysis, the samples were measured in triplicate on previously sonicated diluted dispersions in deionised water. Finally, the elemental composition of the EOCs-functionalised particles was determined by

combustion analysis for C, H and N using a CHNS1100 Elemental Analyser (CE Instruments, UK).

2.4. Toxicological evaluation of EOCs-functionalised MCM-41 microparticles

2.4.1. Cell culture

Human hepatocarcinoma (HepG2) cells were cultured in DMEM-Glutamax medium supplemented with 10% NBCS, 100 U/mL penicillin and 100 μg/mL streptomycin. Cells were maintained in 5% CO_2 humidified incubator at 37ºC. Growth medium was changed every 2–3 days or as required. Cells were subcultured by trypsinisation when about 80% confluence was reached and were used for experiments under 40 subpassages. Absence of mycoplasma contamination was examined regularly in cell cultures with the MycoAlert™ PLUS Myco- plasma kit (Lonza Rockland, USA).

2.4.2. Test solutions

Stock solutions of EOCs were prepared in DMSO (2.5 M) and were maintained at -20 °C until used. Particle suspensions were prepared in DMEM supplemented medium and were sonicated for 10 min immediately prior to use. During the study of the cytotoxic effect of carvacrol and thymol exposure, the final DMSO concentration in the test solutions was below 0.1%. Appropriate negative controls containing the same amount of solvents were included in each experiment. For the analysis of MCM-41 materials, cell-free particle control samples were included for each particle type and concentration and were used to correct particle interference from the test wells when necessary.

2.4.3. MTT assays

Direct exposure cytotoxicity assays

The MTT assay is one of the most commonly used colorimetric assays to evaluate cell viability. In this method, the yellow, positively charged tetrazolium salt enters viable cells, whereupon it is metabolically reduced to the insoluble blue-violet form of formazan by components of the respiratory chain (Rampersad, 2012). This assay was used to determinate the mean inhibition concentration (IC_{50}) values of the EOCs and the EOCs-functionalised silica, and to compare the cytotoxic effect of the functionalised-particles constituents. Briefly, cells were seeded in 96-well plates at a density of 1 x 10^5 and 3 x 10^4 cells/mL for 24-h and 48-h experiments, respectively. After 24 h attachment, cells were exposed to serial dilutions of carvacrol (0.01-2.5 mM), thymol (0.06-1 mM), carvacrol- and thymol-functionalised MCM-41 microparticles (0.01-2.5 mg/mL) and to equivalent concentrations of EOCs, bare and functionalised particles for their comparative analysis (Table 1). The concentration ranges of EOCs and functionalised particles were selected according to previous works (Fuentes et al., 2021). In the comparative studies, concentration ranges were stablished from the IC_{50} values found for carvacrol and thymol, and then the equivalent particle concentrations were calculated from the EOCs content determined by elemental analysis. After a 24-h or 48-h incubation period, wells were washed with 100 µL PBS and 100 µL of 10% MTT stock solution (5 mg/mL in PBS) in supplemented DMEM medium were added per well. Then, plates were incubated in darkness at 37 ˚C, 5% CO_2 for 3 h. After this time, the MTT solution was discarded, wells were washed with PBS and 100 µL of DMSO were added to dissolve formazan crystals. Finally, plates were shaken at 300 rpm for 10 min and absorbance was measured at 570 nm using a MultiSkan EX ELISA plate reader (Thermo Scientific, USA). Cell viability was expressed as a percentage in relation to the negative control (unexposed cells).

Exposure to sublethal concentrations of toxicants trigger adaptative cellular responses linked to their cytotoxicity mechanism (Severin et al., 2017). For this reason, sublethal concentrations ($<IC_{50}$) were used to further investigate the toxicity mechanism underlying to EOCs-functionalised particles exposure. To this end, the IC_{50} values of the particles found in the MTT assay were used to calculate the sublethal concentrations ($IC_{50/2}$, $IC_{50/4}$, $IC_{50/8}$) for the different *in vitro* endpoints: ROS formation, ΔΨm, LPO and apoptotic and necrotic responses.

Table 1. Concentrations assayed in the comparative study of carvacrol, thymol, and bare and EOCs-functionalised MCM-41 microparticles.

	Concentrations			
	A	**B**	**C**	**D**
Carvacrol (mM)	0.25	0.5	1	2
Bare MCM-41 (mg/mL)	4.5	8.9	17.9	35.7
Carvacrol MCM-41 (mg/mL)	4.4	8.8	17.7	35.4
Thymol (mM)	0.25	0.5	1	2
Bare MCM-41 (mg/mL)	3.8	7.7	15.3	30.6
Thymol MCM-41 (mg/mL)	3.7	7.6	15.1	30.3

Extract exposure cytotoxicity assays

An extract dilution exposure method was applied to evaluate a possible cytotoxic effect due to components leached from the surface of the functionalised particles to the culture medium. For this purpose, a stock solution of the carvacrol or thymol-functionalised particles in DMEM supplemented medium (2.5 mg/mL) was vigorously stirred, sonicated in an ultrasonic bath for 10 min, and maintained at 37 ºC for 24 h. After this time, the stock solution was serially diluted (0.01-2.5 mg/mL), and dilutions were filtered using

0.2 μm cellulose acetate filters in order to remove the particles. Then, cells were exposed to the filtered solutions and cytotoxicity of the samples was determined by the MTT assay as described previously.

2.4.4. Lactate dehydrogenase (LDH) activity

The LDH activity was determined using the CyQUANT LDH Cytotoxicity Assay kit (Thermo Scientific, USA) according to the manufacturer's protocol. Briefly, cells were seeded in 96-well plates at 10^5 cells/mL (100 μL/well) and allowed to attach for 24 h. Then, cells were treated with 10 μL of functionalised particles concentrations (0.01-2.5 mg/mL) for a 24 h period. After this time, 10 μL sterile ultrapure water (Spontaneous LDH Activity) or 10 μL lysis buffer (Maximum LDH Release) were added to control wells and plates were incubated in darkness at 37 °C and 5% CO_2 for 45 min. Then, 50 μL of each sample medium was transferred to a new plate and 50 μL of the reaction mixture were incorporated. After incubation at room temperature for 30 min, reactions were ended by adding 50 μL of the stop solution. Absorbance measurements were carried out in a microtiter plate reader at 490 nm. Results were expressed as LDH release (%) in the exposed cells relative to spontaneous and maximum LDH controls.

2.4.5. ROS formation

ROS formation was determined as described by Ruiz-Leal and George (2004). Cells were seeded in black 96-well microplates at 2×10^5 cells/mL density. After 24 h of cell attachment, cells were washed with PBS and 20 μM H_2-DCFDA dye in culture medium were added. Following 20 min incubation in darkness at room temperature, the dye solution was removed and the cells were exposed to different concentrations of the functionalised particles (18.75, 37.5 and 75 μg/mL). Then, fluorescence was measured every 15 min for 2 h at 490 nm excitation and 545 nm emission wavelength on a Wallace

Victor2, model 1420 multilabel counter (PerkinElmer, Finland). The percentage of ROS generation was expressed as the percentage of the fluorescence values obtained compared the negative control (unexposed cells).

2.4.6. Determination of mitochondrial membrane potential

The ΔΨm was determined by the uptake of the green-fluorescent dye Rhodamine 123 upon functionalised microparticles exposure. Cells were seeded at a density of 2×10^5 cells/mL in black 96-well microplates. After 24 h of cell attachment, cells were washed with 100 µl/well PBS and were exposed to 3 different concentrations of the functionalised particles (18.75, 37.5 and 75 µg/mL) in 10% NCBS-supplemented medium for 24 h. Following exposure time, cells were washed with 100 µl/well of PBS and Rhodamine-123 (5 µM) was added in non-supplemented media. After 15 min of incubation at 37°C and 5% of CO_2 in darkness, the dye solution was removed, cells were washed twice and finally resuspended in 200 µl/well PBS. The fluorescence (λexcitation=485 nm, λemission=535 nm) was measured using a microplate reader Wallace Victor2, model 1420 multilabel counter (PerkinElmer, Finland). The results are presented as the percentage of fluorescence of Rhodamine 123 dye in the exposed cells compared to the negative control (unexposed cells).

2.4.7. Lipid peroxidation assays

The effect of sublethal concentrations exposure to functionalised particles on LPO was performed by determining the thiobarbituric acid reactive substances (TBARS) formation, according to the method described by Ferrer et al. (2009). Briefly, 3×10^4 cells/well were seeded in six-well plates, allowed to attach for 24 h and then exposed to functionalised particles (18.75, 37.5 and 75 µg/mL). After 24 h exposure, cells were washed with PBS, homogenised in 150 mM sodium phosphate buffer (NaH_2PO_4) pH 7.4

and lysate with the Ultra-Turrax T8 IKA®-WERKE for 30 s. Cells samples were mixed with 0.5% TBA, 1.5mM DFA and 3.75% BHT and heated at 100 ºC in a boiling water bath for 20 min. After cooling for 5 min, samples were centrifuged at 4000 rpm for 15 min to remove the precipitate. The absorbance of the supernatant was then determined at 535 nm. Simultaneously, the protein content of the samples was measured by the Lowry method using the DC Protein Assay (BIO-RAD Laboratories, USA) at 690 nm wavelength. Results were expressed as ng of malondialdehyde (MDA) per mg of protein.

2.4.8. Apoptosis/necrosis assays

Apoptosis/necrosis analysis was performed by flow cytometry using the FITC Annexin V apoptosis detection kit (BD Biosciences, USA). Briefly, cells were seeded in 6-well plates at a density of 3 x 10^4 cells/well. After attachment, cells were exposed to functionalised particles (18.75, 37.5 and 75 µg/mL) for 24 h. Then, cells were trypsinised, washed twice with ice-cold PBS and resuspended in binding buffer. One hundred µL of cells (1 x 10^5 cells/mL) were stained by adding 5 µl of FITC Annexin V and 5 µl of Propidium Iodide (PI) and incubated at room temperature in darkness for 15 min. After this time, 400 µL of binding buffer were added to each tube and samples were analysed using a BD LSRFortessa flow cytometer (BD Biosciensces, USA). Quadrant statistics were carried out to differentiate between necrotic, early apoptotic and late apoptotic cells. The percentage of cells in each of the categories was calculated by subtracting the number of cells in the control group from the number of cells in the treated population.

2.5. Statistical analysis

Statistical analysis of data was performed using Statgraphics Centurion XVI software package (Statpoint Technologies, Inc., USA). Data were expressed as the mean (SEM) of three independent experiments for each endpoint. Data from the cytotoxicity assays were

transferred to GraphPad Prism version 8.0.1 (GraphPad Software, USA) to adjust the IC_{50} curve by using a four-parameter sigmoidal fit. The statistical analysis of the results was carried out by Student's t-test for paired samples. In the MTT comparative study differences between groups were analysed statistically with one-way ANOVA followed by the Tukey HDS *post-hoc* test for multiple comparisons. The difference level of $p \leq 0.05$ was considered statistically significant.

3. Results

3.1. Physico-chemical characterisation of MCM-41 microparticles

To study the morphology and structure of the bare and carvacrol- or thymol-functionalised MCM-41 particles, TEM analysis was performed. As shown in Figure 1, the three particle types exhibit an irregular external shape and a hexagonal periodic structure of internal channels, in the form of alternate black and white parallel lines, typical of the ordered mesoporous structure of MCM-41 materials (Alothman, 2012; Meynen et al., 2009). These results confirmed that the synthesis process of the MCM-41 materials was correct and that the functionalisation process did not significantly modify the characteristic structure of these materials.

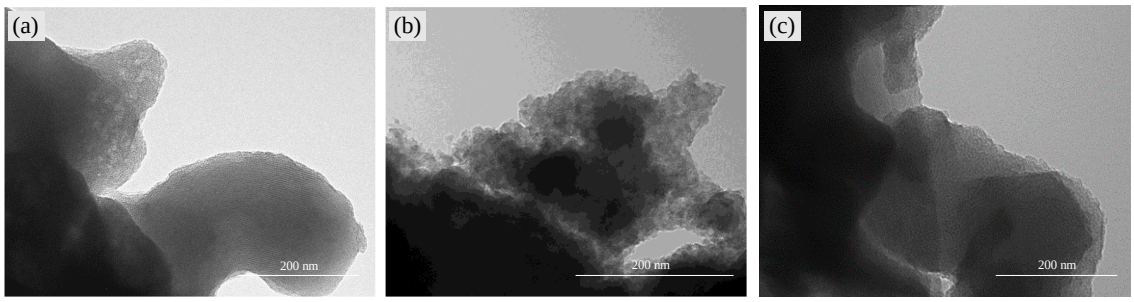

Figure 1. TEM images of bare MCM-41 (a), carvacrol-functionalised MCM-41 (b) and thymol-functionalisedMCM-41 microparticles (c). Scale bar indicates 200 nm.

The zeta potential values and the particle size distribution of the bare and functionalised MCM-41 particles and the carvacrol or thymol content of MCM-41-functionalised materials are depicted in Table 2. The negative zeta potential value observed for bare MCM-41 is related to negatively charged hydroxyl groups on the silica surface. By contrast, functionalised particles displayed positive zeta potential values, evidencing the presence of the carvacrol and thymol alkoxysilane derivatives grafted on their surface. Particle size distribution analysis showed that the three MCM-41 microparticles types were under 700 nm. This value was slightly higher for the bare than functionalised particles, since the higher number of steps included during the functionalisation process has been suggested to reduce the formation of agglomerates (Fuentes et al., 2020). Finally, the quantification of carvacrol and thymol grafted on the particles surface was determined by elemental analysis. Small differences were found in the reaction yield for both types of EOCs, the content of thymol immobilised on the surface of MCM-41 functionalised microparticles being slightly higher than carvacrol (Table 2). These results were used to establish the equal concentrations of free EOCs and functionalised particles for the comparative cell viability assays (Table 1).

Table 2. Zeta potential (ZP) values, particle size distribution ($d_{0.5}$) and EOC content (α) of the different MCM-41 microparticles.

Type of particle	ZP (mV)	$d_{0.5}$ (µm)	α (g/g_{SiO2})
Bare MCM-41	-33.43 (0.84)	0.68 (0.00)	
Carvacrol-MCM-41	27.40 (2.06)	0.62 (0.00)	0.0084
Thymol-MCM-41	21.1 (1.74)	0.65 (0.00)	0.0098

ZP and $d_{0.5}$ values are expressed as mean (SD) (n = 3).

306

307 **3.2. Toxicological evaluation of EOCs-functionalised MCM-41 microparticles**

308 **3.2.1. MTT assays**

309 Firstly, the cytotoxic effect of carvacrol and thymol was determined after 24 h and 48
310 h exposure of HepG2 cells, as determined using the MTT assay. Both components
311 reduced cell viability in a time and concentration-dependent manner (Fig. S1 and S2).
312 Carvacrol was slightly less cytotoxic than thymol, when cells were exposed to the EOCs
313 for 24 h; however, no differences were found after 48 h incubation-period. The IC_{50}
314 values found after 24 h exposure were 0.45 (0.01) mM and 0.40 (0.03) mM for carvacrol
315 and thymol, respectively. At 48 h, the IC_{50} value for both components was similar (0.32
316 (0.02) mM for carvacrol and 0.32 (0.03) mM for thymol).

317 Figure 2 displays the cytotoxicity-response curves for carvacrol and thymol-
318 functionalised MCM-41, either directly added to the culture medium or in an extract
319 dilution form. Both materials reduced cell viability in a concentration-dependent manner
320 (Fig. S3) when HepG2 cells were directly exposed to the functionalised particles for 24 h
321 and 48 h, as measured by the MTT assay. The IC_{50} values found for carvacrol-
322 functionalised MCM-41 were 0.15 (0.01) mg/mL and 0.09 (0.04) mg/mL for 24 h and 48
323 h, respectively. Thymol-functionalised microparticles showed an IC_{50} value of 0.15 (0.08)
324 mg/mL after 24 h of cells' exposure and 0.11 (0.08) mg/mL after 48 h. However, when
325 cells were treated with the filtered medium which previously contained each type of
326 particle, cell viability was significantly higher. A cell viability of 75% and 78% for
327 carvacrol- and thymol-functionalised silica, respectively, were observed after 24 h
328 exposure to the highest concentrations tested (2.5 mg/mL). After 48 h of treatment, these
329 percentages were 92% in the case of carvacrol-functionalised particles, and 85% in the

case of thymol-functionalised silica. Indeed, when cells were exposed to the filtered solutions equivalent to the IC_{50} values found for both types of functionalised particles, cell viability remained around 100%.

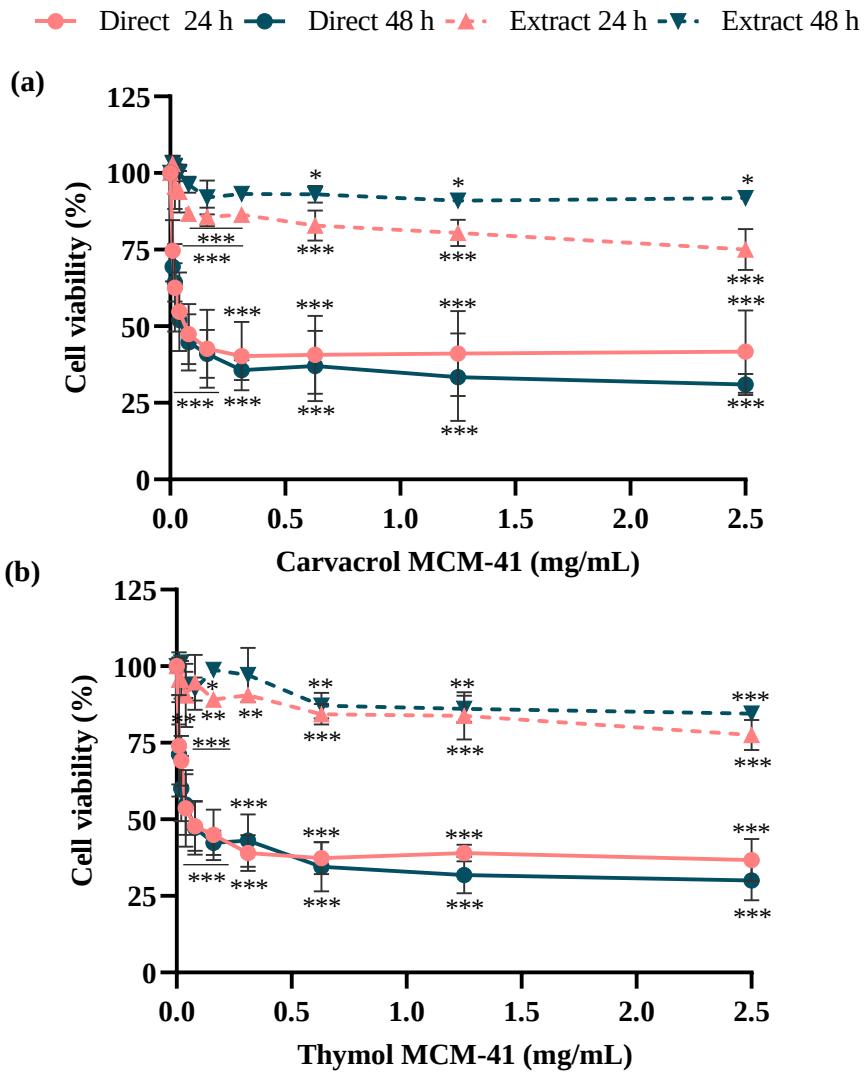

Figure 2. Concentration-cell viability plots of HepG2 cells exposed either directly or in an extract dilution form to carvacrol-functionalised MCM-41 (a); and thymol-functionalised MCM-41 (b) for 24 h and 48 h by the MTT assay. Each bar represents the mean (SEM) of three independent assays, each performed 6-fold. (*) $p \leq 0.05$; (**) p

339 ≤ 0.01; (***) $p \leq 0.001$ indicates significant differences compared to the control according
340 to the Student's t-test.

341

342 The IC_{50} values previously found for carvacrol and thymol were used to define the
343 concentration range for the comparative analysis of the cytotoxic effects free EOCs, EOC-
344 functionalised MCM-41 and bare MCM-41 microparticles. The results of the comparative
345 analysis are shown in Figure 3. Free carvacrol was significantly less cytotoxic than
346 equivalent concentrations of carvacrol anchored on the surface of silica microparticles at
347 the two lowest concentrations assayed (0.25 and 0.5 mM). Differences in cell viability
348 between free carvacrol and carvacrol-functionalised MCM-41 ranged from 75% to 32%
349 and from 61% to 24% after 24 h and 48 h exposure, respectively. Bare MCM-41
350 microparticles also showed a lower cytotoxic response than equivalent concentrations of
351 functionalised materials at the three highest concentrations tested for both times of
352 exposure. Differences in cell viability between bare MCM-41 and carvacrol-
353 functionalised MCM-41 range from 75% to 47% and from 89% to 47% after treating cells
354 for 24 h and 48 h, respectively.

355 Regarding thymol, the free compound was significantly less cytotoxic than the
356 equivalent concentration of immobilised compound on MCM-41 microparticles at the
357 highest concentration tested (0.25 mM). At this concentration, differences in cell viability
358 between free thymol and thymol-functionalised MCM-41 where of 59% and 61% after
359 24 h and 48 h exposure, respectively. Bare MCM-41 was found less cytotoxic than
360 thymol-functionalised MCM-41 at the 0.25 mM and 0.5 mM concentrations. At these
361 concentrations, differences in cell viability between both types of particles ranged from
362 65 % to 44 % and from 61 % to 55 % after 24 h and 48 h exposure, respectively.

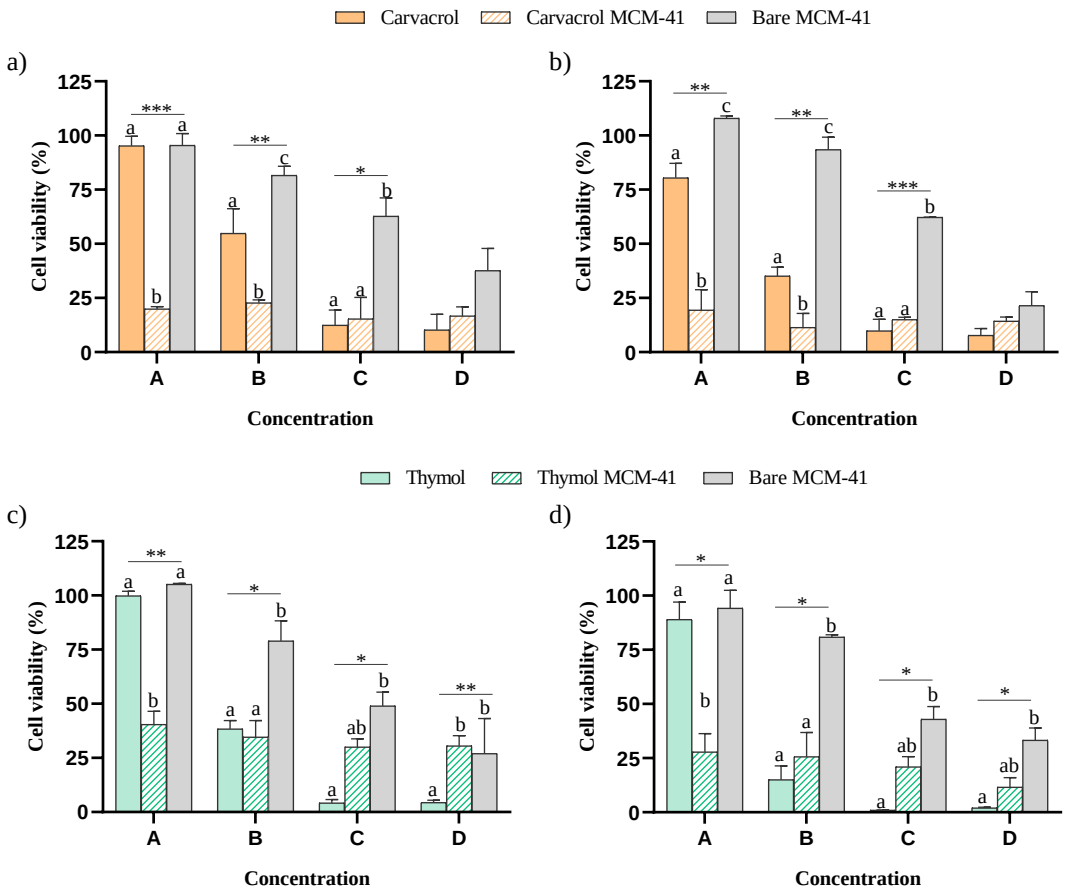

363

364 **Figure 3.** Concentration-cell viability plots of HepG2 cells exposed to equivalent
365 concentrations of carvacrol, carvacrol functionalised MCM-41 and bare MCM-41 for 24
366 h (a) and 48 h (b) or to equivalent concentrations of thymol, thymol functionalised MCM-
367 41 and bare MCM-41 for 24 h (c) and 48 h (d). Each bar represents the mean (SEM) of
368 three independent assays, each performed 6-fold. Significant differences (***$p \leq 0.01$,
369 **$p \leq 0.01$, *$p \leq 0.05$) are indicated by different letters (a–c).

370

371 **3.2.2. LDH assay**

372 The LDH assay measures the activity of LDH released in cell culture medium after
373 exposure to cytotoxic substances, as an indicator of irreversible cell death due to cell
374 membrane damage (Aslantürk, 2018). Therefore, higher LDH values in the medium

indicate higher toxicity levels. Figure 4 depicts the effect of EOCs-functionalised particles on LDH release into the medium after 24 h exposure. As shown in this figure, carvacrol and thymol-functionalised silica exposure resulted in a significant increase of LDH release compared to controls at the highest concentrations tested. Exposure to 2.5 mg/mL of carvacrol-functionalised silica increased the LDH release more than 10% compared to the control. For thymol-functionalised silica at the two highest concentrations tested (1.25 and 2.5 mg/mL), the LDH leakage into the culture medium increased by 14 % and 16%, respectively. No differences were observed at all the other tested concentrations respect to the control.

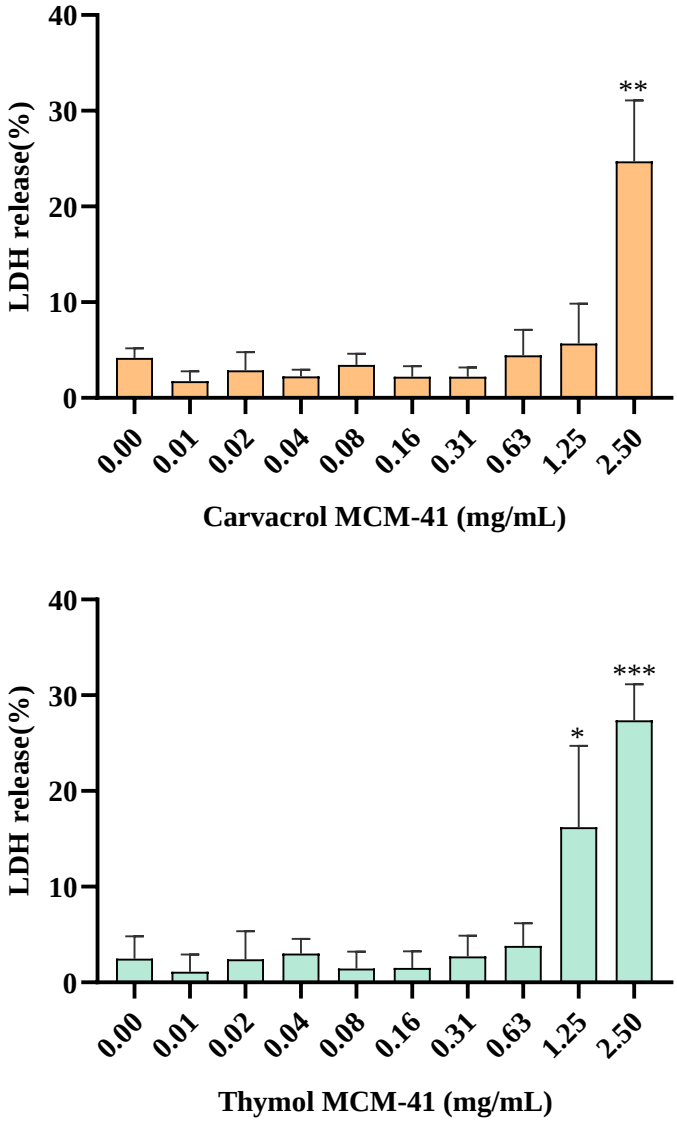

385

386 **Figure 4.** LDH activity in HepG2 cells exposed to carvacrol-functionalised MCM-41
387 microparticles (a) and thymol-functionalised MCM-41 microparticles (b) for 24 h.
388 Results are expressed as mean (SEM, n=3). (*) $p \leq 0.05$; (**) $p \leq 0.01$; (***) $p \leq 0.001$
389 indicates significant differences compared to the control according to the Student's t-test.

390

391 **3.2.3. ROS formation**

392 The formation of ROS was studied as an indicator of oxidative stress using the
393 fluorescein derivative H_2DCF-DA. Figure 5 shows ROS production on HepG2 cells

394 exposed to 18.75, 37.5 and 75 µg/mL of carvacrol- and thymol- functionalised MCM-41
395 microparticles over 120 min post exposure. As can be observed, exposure to the three
396 concentrations of both types of functionalised particles did not induce the formation of
397 ROS over this time period, since no significant differences in the DCFDA dye
398 fluorescence intensity was observed compared to the control cells.

399

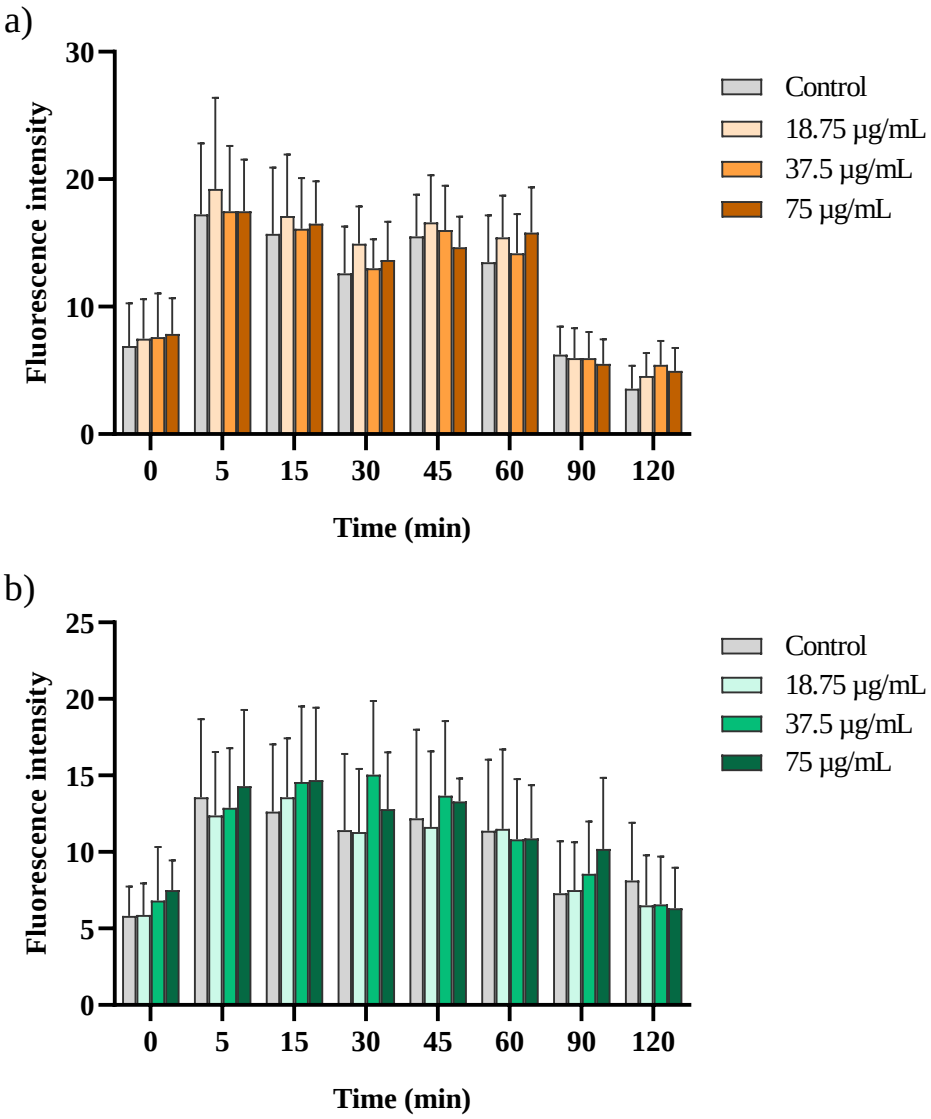

400

401 **Figure 5.** ROS induction as a function of time (0-120 min) in HepG2 cells exposed to
402 sublethal concentrations of carvacrol-functionalised MCM-41 microparticles (a) and

403 thymol-functionalised MCM-41 microparticles (b). Results are expressed as mean (SEM,
404 n=3). No significant differences were found between the different test solutions and the
405 control.

406

407 **3.2.4. Lipid peroxidation assays**

408 The MDA levels were measured as an indicator of LPO and oxidative stress using the
409 TBARS assay. The LPO production on HepG2 cells in the presence of carvacrol and
410 thymol-functionalised silica at 18.75, 37.5 and 75 μg/mL can be observed in Figure 6.
411 The results obtained demonstrated that 24 h of exposure to carvacrol-functionalised
412 particles caused a significant increase in MDA production by 44% (18.75 μg/mL), 15%
413 (37.5 μg/mL) and 54% (75 μg/mL) with respect to control cells. Similarly, 24-h exposure
414 to thymol-functionalised particles significantly increased MDA levels in a concentration-
415 dependent manner (Fig. 6). Exposure to 18.75, 37.5 and 75 μg/mL of thymol-
416 functionalised MCM-41 for 24 h resulted in an increase of 17%, 24% and 55%,
417 respectively, compared to the control.

418

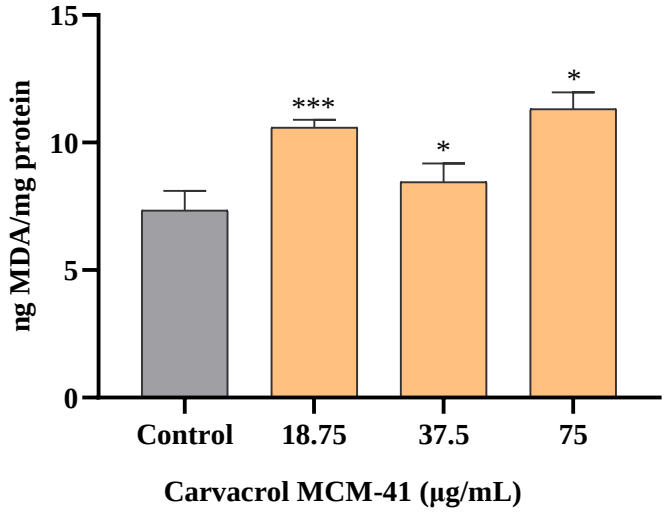

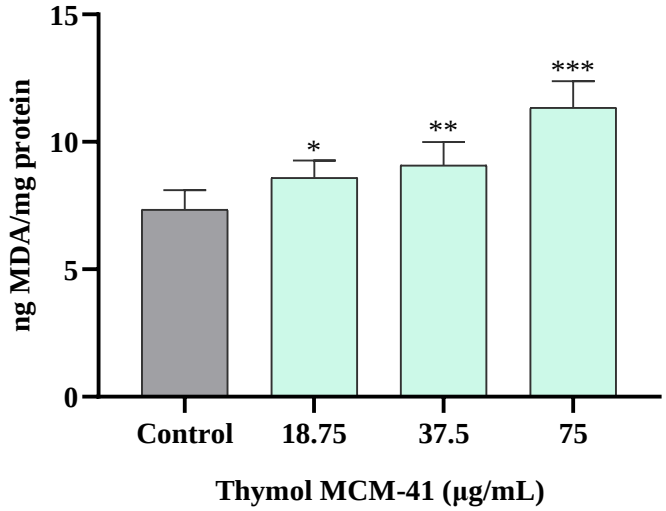

419

420 **Figure 6.** Effect on LPO as measure by MDA production after HepG2 cells exposure to
421 sublethal concentrations of carvacrol-functionalised MCM-41 microparticles (a) and
422 thymol-functionalised MCM-41 microparticles (b) for 24 h. Results are expressed as
423 mean (SEM, n=3). (*) $p \leq 0.05$; (**) $p \leq 0.01$; (***) $p \leq 0.001$ indicates significant
424 differences compared to the control according to the Student's t-test.

425

426 **3.2.5. Determination of ΔΨm**

To assess whether functionalised particles exposure affected mitochondrial function, potential changes in ΔΨm were analysed by employing the mitochondria fluorescent dye Rhodamine 123. As shown in Figure 7, exposure to both materials for 24 h induced significant ΔΨm decrease in a concentration-dependent manner. This effect was higher for carvacrol-functionalised particles that decreased ΔΨm at the two highest concentrations tested, 37.5 µg/mL and 75 µg/mL, by a 19% and 28% with respect to the control, respectively. Thymol-functionalised particles in a 75 µg/mL concentration resulted in a significant decrease of ΔΨm by a 24% when compared to untreated control cells.

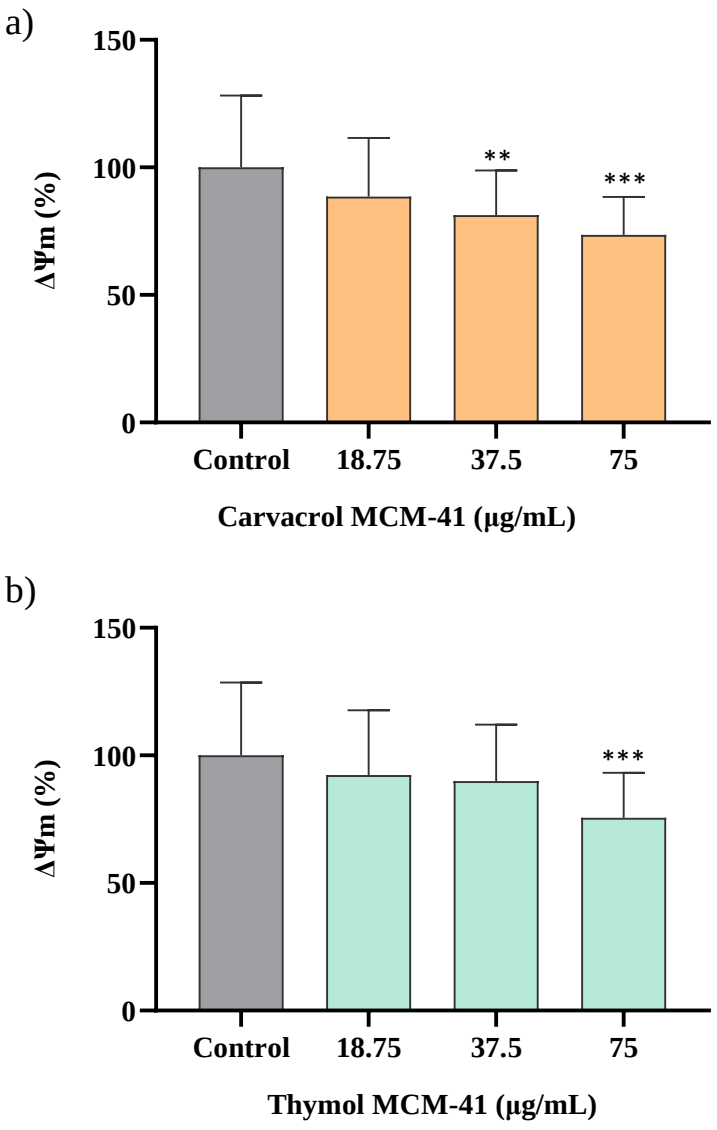

Figure 7. Effect on mitochondrial membrane potential (ΔΨm) after HepG2 cells exposure to sublethal concentrations of carvacrol-functionalised MCM-41 microparticles (a) and thymol-functionalised MCM-41 microparticles (b) for 24 h. Results are expressed as mean (SEM, n=3). (**) $p \leq 0.01$; (***) $p \leq 0.001$ indicates significant differences compared to the control according to the Student's t-test.

3.2.6. Apoptosis and necrosis assays

Flow cytometry analysis was applied with the aim to determine the related death mechanism underlying the cytotoxic effect observed for functionalised materials. The fluorescein Annexin V-FITC/PI double staining was used to distinguish and quantify the percentage of necrotic, early apoptotic and late apoptotic cells after exposure to sublethal concentrations of carvacrol and thymol-functionalised MCM-41 (Fig. 8 and Fig. 9, respectively). The results revealed an increase in the percentage of necrotic, early apoptotic and late apoptotic cells following treatment with increasing concentrations of both functionalised particles. However, only significant differences were found between control cells and cells exposed to the highest concentrations tested of both materials (75 µg/mL). The basal necrotic population in the control was 2.76 (0.40) %. After treatment with 75 µg/mL of carvacrol and thymol-functionalised particles for 24 h, the necrotic rate raised to 10.20 (3.82) % and 8.63 (3.54) %, respectively. The percentage of early apoptotic HepG2 cells underwent an increase from 6.65 (1.73) % in control unexposed cells to 15.90 (3.46) % and 13.31 (1.83) % for carvacrol and thymol-functionalised MCM-41 in that order. Similarly, the percentage of late apoptotic cells augmented from 8.16 (0.26) % in the untreated culture to 16.27 (0.20) % and 13.98 (2.18) % for carvacrol and thymol-functionalised particles exposed cells, respectively.

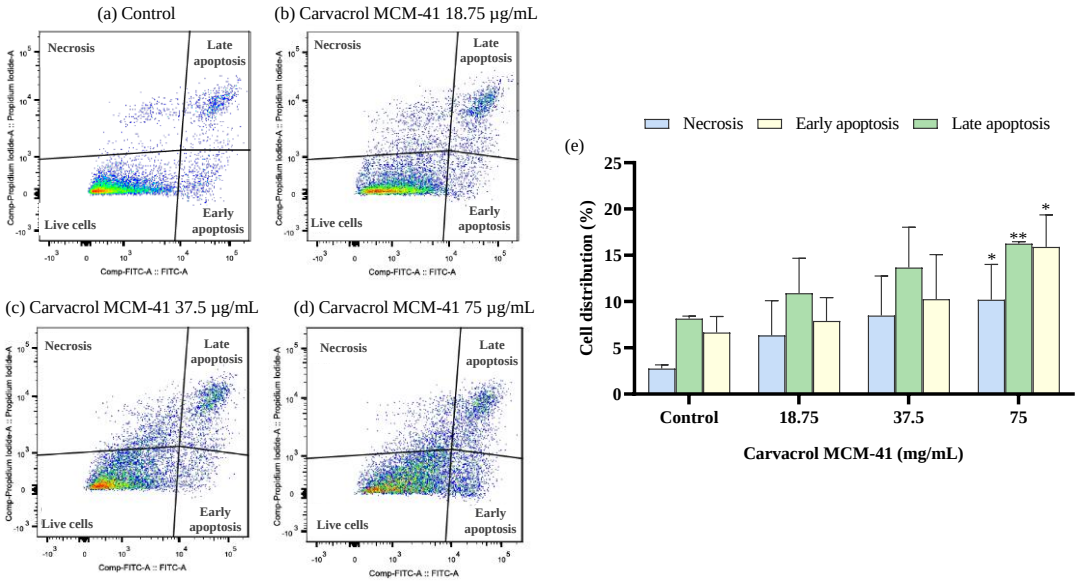

Figure 8. Flow cytometry analysis of apoptotic and necrotic HepG2 cells exposed to sublethal concentrations of carvacrol-functionalised MCM-41 microparticles using Annexin V-FITC/PI double staining. Representative two-dimensional dot plot diagrams of three independent experiments for (a) untreated cells; (b) cells treated with 18.75 µg/mL; (c) 37.5 µg/mL; (d) and 75 µg/mL of carvacrol-functionalised MCM-41 microparticles. The upper left quadrant (PI+/Annexin V-FITC-) represents necrotic cells, the left lower quadrant (PI-/Annexin V-FITC-) represents live cells, the upper right quadrant (PI+ /Annexin V-FITC+) represents late apoptotic cells and the lower right quadrant (PI-/Annexin V-FITC+) represents early apoptotic cells. (e) Percentage of early apoptotic, late apoptotic and necrotic cells. Results are expressed as mean (SEM, n=3). (*) $p \leq 0.05$; (**) $p \leq 0.01$ indicates a significant difference compared to the control according to the Student's t-test.

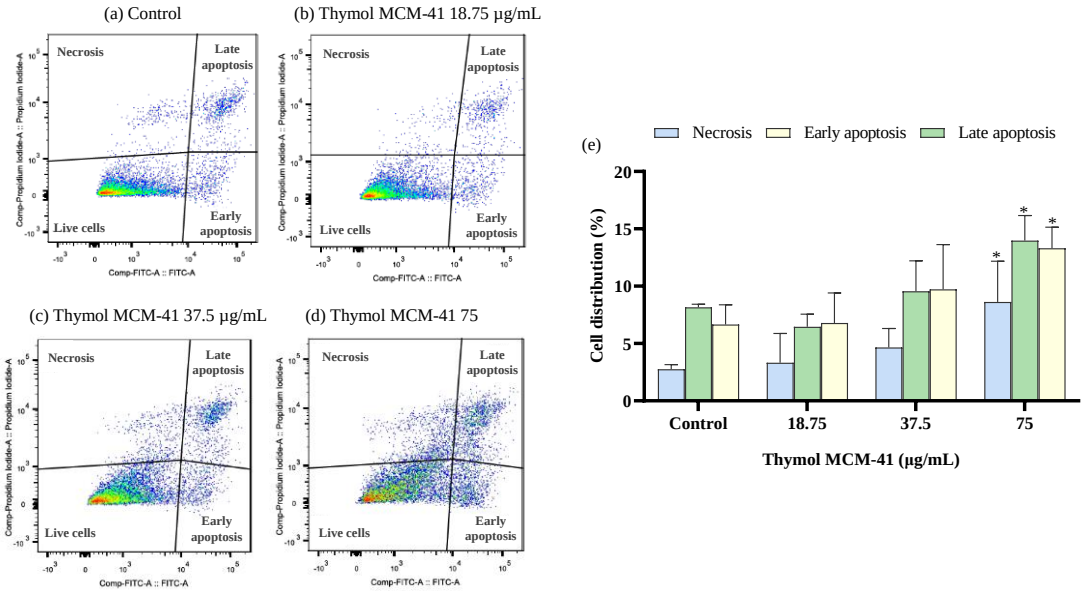

Figure 8. Flow cytometry analysis of apoptotic and necrotic HepG2 cells exposed to sublethal concentrations of thymol-functionalised MCM-41 microparticles using Annexin V-FITC/PI double staining. Representative two-dimensional dot plot diagrams of three independent experiments for (a) untreated cells; (b) cells treated with 18.75 µg/mL; (c) 37.5 µg/mL; (d) and 75 µg/mL of thymol-functionalised MCM-41 microparticles. The upper left quadrant (PI+/Annexin V-FITC-) represents necrotic cells, the left lower quadrant (PI-/Annexin V-FITC-) represents live cells, the upper right quadrant (PI+ /Annexin V-FITC+) represents late apoptotic cells and the lower right quadrant (PI-/Annexin V-FITC+) represents early apoptotic cells. (e) Percentage of early apoptotic, late apoptotic and necrotic cells. Results are expressed as mean (SEM, n=3). (*) $p \leq 0.05$ indicates a significant difference compared to the control according to the Student's t-test.

4. Discussion

The immobilisation of natural EOCs on the surface of silica particles has emerged as an innovative technology to enhance their antimicrobial and antioxidant properties.

However, due to their possible application in food or food contact materials, their safety needs to be addressed. For this purpose, the potential health hazards derived from exposure to these new materials for consumers' health should be thoroughly investigated at the cellular level. The use of cell cultures is a relevant tool in toxicity testing to enhance our understanding of hazardous materials and to predict their effects on human health (Eisenbrand et al., 2002). Assays to determine basal cytotoxicity measure cell viability or cell death as a consequence of damage to basic cellular functions, and allow for a rapid identification of toxic compounds. Moreover, *in vitro* tests on specialised cell functions and metabolic endpoints give insight into the pathways and mechanisms of action involved in chemically induced toxicity at both the molecular and the cellular level. This study examines the *in vitro* toxic effect of carvacrol and thymol-functionalised MCM-41 silica particles on HepG2 cells as model cell line. The aim was to evaluate their potential toxicity and to fully understand the associated mechanism involved.

First, a comparative analysis of the functionalised-particles and their constituents was carried out, revealing that free EOCs and bare MCM-41 microparticles exhibited significantly milder cytotoxic effects than equivalent concentrations of EOC-functionalised silica. Similar results were previously found for eugenol and vanillin-functionalised MCM-41 microparticles (Fuentes et al., 2021). In that study, the stronger cytotoxic effect observed for the EOCs-functionalised silica was attributed to physico-chemical properties, such as surface charge and hydrophobicity that could be responsible for promoting interactions of EOCs with cell membranes. Also, Chen et al. (2009) found that functionalisation with carvacrol increased the cytotoxicity of chitosan nanoparticles in a 3T3 mouse fibroblast cell line. The IC_{50} value observed for carvacrol-grafted chitosan nanoparticles was around 1 mg/mL, whereas at a 2 mg/mL concentration of unmodified chitosan nanoparticles cell viability was still higher than 80%, as measured by the MTT

assay. However, carvacrol-modified chitosan nanoparticles were significantly less cytotoxic towards mammalian cells than free carvacrol. As previously reported, this discrepancy may be the result of differences in the starting material, the cell type employed for the cytotoxicity assays or the lesser degree of grafting achieved for the silica particles (Fuentes et al., 2021).

Cytotoxicity data may serve to predict acute systemic toxicity *in vivo* and also to define the concentration range for mechanistic toxicity studies (Ciappellano et al., 2016; Severin et al., 2017). With this twofold objective, the cytotoxicity of carvacrol- and thymol-functionalised microparticles was analysed by two methods based on different physiological endpoints; the MTT and the LDH release assays. As measured by the MTT method, 24 h exposure resulted in an IC_{50} value of 0.15 mg/mL for both functionalised materials, and this value decreased to 0.09 mg/mL and 0.11 mg/mL after 48-h treatment, for carvacrol- and thymol-silica, respectively. In a previous work, Fuentes et al., 2021 determined the cytotoxic effect of bare MCM-41 silica microparticles on HepG2 cells by the MTT assay and confirmed the biocompatibility reported for calcined mesoporous silica (Aburawi et al., 2012; Al-Salam et al., 2011; Samri et al., 2012; Shamsi et al., 2010). Exposing cells to bare MCM-41 silica for 24 h and 48 h resulted in IC_{50} values of 18.90 mg/mL and 15.82 mg/mL, respectively (Fuentes et al., 2021). By comparison with these results, herein we found that functionalisation of MCM-41 microparticles with carvacrol or thymol increase cytotoxicity of the starting material approximately 100-fold. However, when cells were exposed to the filtered medium which previously contained the particles during the extract dilution assays, we found that at the IC_{50} values calculated for both materials, the cell viability remained around 100%. These results may be interpreted as a confirmation of a direct interaction of cells with the particles being responsible for the cytotoxic behaviour found for both, carvacrol- and thymol-functionalised particles, while

543 an indirect cytotoxicity effect due to components leached from the surface of the
544 functionalised particles or by means of depletion of nutrients from the culture medium
545 (Casey et al., 2008) is not expected.

546 Cytotoxic effects assessed by the LDH assay were observed at higher particle
547 concentrations than with the MTT assay, thus, demonstrating that the MTT assay was
548 more sensitive than the LDH assay for determining cell viability after EOCs-
549 functionalised microparticles exposure. The sensitivity of the different cytotoxicity assays
550 has been demonstrated to differ depending on the mechanisms that lead to cell death
551 (Weyermann et al., 2005). The MTT method determines mitochondrial metabolic activity
552 of viable cells, while LDH assay measures cell death due to cell membrane damage. In
553 this sense, the differences observed between both assays concerning their sensitivity may
554 suggest that impairment of mitochondrial function may precede disruption of the
555 membrane integrity and cell lysis in cells exposed to carvacrol and thymol-functionalised
556 microparticles. Moreover, these results support the widespread consensus than more than
557 one cell viability assay should be used in order to increase the reliability of the results
558 during *in vitro* studies (Aslantürk, 2018; Eisenbrand et al., 2002; Fotakis and Timbrell,
559 2006).

560 It is worth mentioning that different studies have described particle interference when
561 testing cytotoxicity with both methods (Holder et al., 2012; Kroll et al., 2012). Different
562 factors have been proven to limit the sensitivity of the MTT method, including pH, optical
563 activity or surface reactivity of the particles (Abbasi et al., 2021; Laaksonen et al., 2007).
564 In the LDH assay, different inorganic particles have been demonstrated to interfere with
565 this assay by either adsorbing or inactivating the LDH protein, both mechanisms causing
566 a decreased absorbance in the LDH assay and resulting in a false indication of a nontoxic
567 response (Holder et al., 2012). Moreover, Korhonen et al. (2016) used the LDH assay to

568 evaluate the cytotoxic effect of mesoporous silica microparticles in human corneal
569 epithelial (HCE) and retinal pigment epithelial (ARPE-19) cells and found an increased
570 or decreased reactivity in the LDH assay depending on the cell culture medium used.
571 Herein, the MTT and LDH viability assays were also performed under cell-free conditions
572 in order to evaluate interference of the functionalised particles with both assays. At low
573 concentrations, EOCs-functionalised materials did not induce any non-specific response
574 in the MTT and LDH viability assays, while at concentrations higher than 0.31 mg/mL
575 of particles, significantly increased absorbance was observed for both cell-free assays.
576 Consequently, data were corrected to avoid any particle interferences by subtracting the
577 absorbance of the cell-free controls from that of the test wells.

578 In order to gain insight into the cytotoxicity mechanism induced by these materials,
579 different endpoints related to oxidative stress, mitochondrial dysfunction and cell death
580 pathway were investigated. In this aspect of the work, the IC_{50} values found for both
581 materials by the MTT assay were used to define the concentration range for further assays.

582 Oxidative stress is a major mechanism involved in toxicity induced by many xenobiotics
583 (Zhang, 2018). It is a result of an imbalance between the production of oxidising
584 molecular species and the protective mechanisms produced by the cells for their removal.
585 ROS are oxygen-containing chemically-reactive molecules that, under normal conditions,
586 are produced by the cells as a consequence of aerobic metabolism (Ray et al., 2012).
587 However, the over production and accumulation of ROS due to interactions of cells with
588 toxic agents may lead to dysfunction of the antioxidant system and oxidative damage to
589 cellular macromolecules such as lipids, proteins or nucleic acids, causing severe cell
590 toxicity (Eisenbrand et al., 2002). To evaluate whether oxidative stress was involved in
591 carvacrol- and thymol-functionalised MCM-41 cytotoxicity, two different biomarkers
592 were used: ROS production and LPO generation. Results showed that exposure to

sublethal concentrations of both materials did not induce early ROS formation as measured by the DCFDA assay. However, a significant increase in MDA levels was found when cells were exposed to the particles for 24 h, indicating that oxidative stress occurred through LPO.

High levels of ROS that persist for a long period are thought to be the major factor responsible for reacting with the polyunsaturated fatty acids of lipid membranes and inducing LPO (Barrera, 2012). The absence of ROS in this study may be explain by differences in the exposure times employed between both assays. The ROS formation was measured within 2 h after exposure to sublethal concentrations of the functionalised silica, while LPO was determined when cells were treated with these materials for 24 h. Accordingly, Santos et al. (2010) evaluated ROS production followed exposure to different mesoporous silicon microparticles in the human colon carcinoma cell line Caco-2 using the DCFDA assay. These authors found no significant increases in hydrogen peroxide concentration or mitochondrial superoxide after 3 h-incubation time but a significant increase in hydrogen peroxide formation after 24 h exposure. Longer exposure times than those usually employed with this method have also been found necessary to detect oxidative stress caused by other toxic insults (Aranda et al., 2013). Some authors also suggest that, although the DCFDA probe has been extensively employed as a biomarker for oxidative stress and is supposed to reflect the overall oxidative status of the cell, it can only detect hydrogen peroxides, peroxyl radicals and peroxynitrite anions and not all the different types of ROS (Herzog et al., 2009).

Toxic agents can generate ROS by directly interacting with the electron-transport chain complexes in the inner mitochondrial membrane (Boelsterli, 2007). Moreover cell-particle interactions can induce ROS formation by a surface- catalysed reaction (Lehman et al., 2016). Indeed, silica particles have been demonstrated to induce ROS formation by

618 both mechanism; by direct contact of cell membrane with the particles surface and by
619 triggering cell-signalling pathways that initiate cytokine release and apoptosis within the
620 cells (Hamilton et al., 2008). Different phenomena including hydrophobic or hydrophilic
621 interactions, active electron configurations, redox potential or semiconductor and
622 electronic properties may be responsible for ROS generation upon interactions of
623 particles with biological systems (Santos et al., 2010). In line with this, Lehman et al.
624 (2016) studied the free radical species generated from the surface of non-porous and
625 mesoporous nanoparticles by electron paramagnetic resonance spectroscopy. These
626 authors found a correlation between ROS released from the nanoparticle surface,
627 intracellular ROS and cellular toxicity in the murine macrophage cell line RAW 264.7.
628 Moreover, amine-functionalisation reduced the amount of free radical generated at the
629 solid–liquid interface by non-porous nanosilica and, as suggested by the authors, this
630 would mitigate their toxic behaviour. Similarly, Santos et al. (2010) also found surface
631 chemistry as a determinant factor that determines ROS production and cell–particle
632 interactions. According to their work, thermally carbonised particles induced toxicity as
633 a result of stimulation of ROS production on Caco-2 cells, while thermally oxidised
634 particles did not induce significant ROS formation and resulted in less damage to cells as
635 a result of weak cell–particle interactions. In our work, the increased cytotoxicity found
636 for the EOCs-functionalised compared to the native microparticles may be attributed to
637 differences in the surface properties between bare and EOCs-functionalised particles,
638 since no differences of size and shape were observed. Cationic nature and hydrophobic
639 surfaces have been demonstrated to increase *in vitro* toxicity and the number of apoptotic
640 cells as a result of strong cell–particle interactions (Saei et al., 2017; Santos et al., 2010).
641 These properties may therefore be related to the increased cytotoxicity found for the
642 functionalised materials in our study.

643 A close relationship exists between ROS formation and mitochondria, since these
644 organelles are considered the main source of ROS in the cell and at the same time
645 mitochondrial damage by ROS formation is a main mechanism of toxicant-induced
646 cytotoxicity (Zhang, 2018). Accordingly, mitochondrial dysfunction is one of the most
647 sensitive indicators of adverse cell effects and it can be evaluated by monitoring changes
648 in ΔΨm of exposed cells (Xu et al., 2004). In this study, a depletion of the ΔΨm was
649 observed after treatment of HepG2 cells with carvacrol and thymol-functionalised silica.
650 The ΔΨm generated is an essential component in a range of processes including energy
651 storage during oxidative phosphorylation, calcium homeostasis or cellular differentiation.
652 Moreover, disruption of mitochondrial integrity has been described as one of the early
653 events leading to apoptosis and may serve as a biomarker for apoptotic cell death (Jeong
654 and Seol, 2008).

655 Exposure to cytotoxic agents can lead to cell death mainly by two major mechanisms:
656 apoptosis and necrosis. In this work, the death mechanism related to the cytotoxic effects
657 induced by modified-MCM-41 exposure was evaluated using the Annexin V-FITC/PI
658 double staining and flow cytometry analysis. This method allows to discriminate between
659 healthy, early apoptotic, late apoptotic and necrotic cells. We found that all three, early
660 apoptotic, late apoptotic and necrotic rates significantly increased after treating HepG2
661 cells to the highest sublethal concentration of both carvacrol and thymol-functionalised
662 silica for 24 h. According to these results, both mechanisms of cell death are involved in
663 the cytotoxicity induced by EOCs-functionalised MCM-41.

664 Apoptosis or programmed cell death is a slow form of cell death that can occur under
665 normal physiological conditions or may be induced by apoptotic compounds. There exist
666 two main pathways that lead to apoptosis: the extrinsic or death-receptor pathway that is
667 activated from outside the cell by ligation of transmembrane death receptors, and the

intrinsic or mitochondrial pathway that begins with the permeabilisation of the mitochondrial outer membrane triggered by different signals such as DNA damage, ischemia or oxidative stress (Wang and Youle, 2009). Depletion of ΔΨm causes the release of mitochondrial intermembrane space proteins into the cytoplasm, including cytochrome c, that consequently triggers other apoptotic factors such caspases activation or chromosome fragmentation, leading to apoptosis through the mitochondrial or intrinsic pathway apoptotic death pathway (Tait and Green, 2013). Therefore, loss of ΔΨm serves as a biomarker for apoptotic cell death.

In contrast to apoptosis, necrosis consists in a rapid form of cell death that is induced by external injuries such as hypothermia, radiation, hypoxia or chemicals that damage the cell membrane (D'Arcy, 2019). Destruction of the plasma membrane or the biochemical supports of its integrity leads to the release of intracellular material, local inflammatory responses, and cell swell and lysis (Miret et al., 2006). In consequence, necrosis can be measured by the presence of the cytoplasmic content in the extracellular fluid i.e. by measuring the activity of enzymes such as LDH. As already explained, the LDH assay was far less sensitive that the MTT assay for evaluating the basal cytotoxicity on HepG2 cells as a consequence of the microparticles exposure, suggesting impairment of the mitochondrial activity rather than cell membrane disruption. As a result, we hypothesise that apoptosis is the most likely mechanism of cell death after EOCs-functionalised particles exposure.

According to our results, the mechanism underlying the cytotoxic effect of carvacrol and thymol-functionalised silica microparticles on HepG2 cells involves induction of oxidative stress that will cause mitochondrial dysfunction and lead to activation of the apoptotic death pathway. This mechanism of toxic action bears similarities with the mechanism described for their constituents. Essential oils and their components have been

693 demonstrated to induce toxicity in eukaryotic cells due to a phenolic-like prooxidant
694 mechanism (Bakkali et al., 2008). These components will penetrate cells and permeabilise
695 cytoplasmic and especially mitochondrial membranes. Then, damaged mitochondria
696 produce ROS, generating reactive phenoxyl radicals with prooxidant potential that may
697 oxidise EOCs. Ultimately, this sequence of events leads to cell death by apoptosis
698 (Bakkali et al., 2008). For their side, different size MCM-41 and SBA-15 microparticles
699 induced ROS formation, especially O_2^-, at concentrations over 1 mg/mL after 3 h
700 incubation on Caco-2 cells, overwhelming the antioxidant defences and causing
701 mitochondrial dysfunction and increasing the apoptotic signalling (Heikkilä et al., 2010).
702 Moreover, as found herein for the EOCs-functionalised silica, metabolic activity was a
703 more sensitive endpoint as measured by ATP depletion, than cell membrane integrity
704 (Heikkilä et al., 2010). However, both bare MCM-41 microparticles and EOCs exhibit
705 cytotoxic effects and ROS generation at much higher concentrations that those found for
706 the functionalised particles object of this study. Our results suggest that either a
707 synergistic effect by the presence on the functionalised particles surface of both, silanol
708 groups from the bulk material and EOCs derivatives from the functionalisation process,
709 either a boosting effect of the EOCs as a consequence of their higher density or reduced
710 volatility, increasing EOCs-cell membrane interactions (Fuentes et al., 2021). Another
711 possible explanation is that EOCs in their free form can be partly metabolised by cells
712 and this phenomenon is not possible for immobilised compounds. However, the cellular
713 uptake of the microparticles by HepG2 cells would still need to be confirmed by confocal
714 microscopy analysis in the future.

715 Alternatives to synthetic preservatives for food applications are not free from potential
716 toxicological hazards. As observed in this work, toxicity studies are necessary for the
717 understanding of the interactions of new materials with biological systems and to

guarantee their safety for human health. In summary, our results show that functionalisation of silica MCM-41 microparticles with the natural EOCs carvacrol and thymol increased the cytotoxic potential of these materials compared to their free constituents. Both particle types behaved similarly in regard to their cytotoxic effects that were proven to emerge from the microparticles themselves and not from degradation products released to the culture media. Overall, the results found in this study support the hypothesis that carvacrol- and thymol-functionalised MCM-41 induced toxicity on HepG2 cells by an oxidative stress-related mechanism. A direct physical interaction between the particles surface and cell membranes could be responsible to induce ROS overproduction. The oxidative stress would lead to oxidation of different cellular components such as lipids and to $\Delta\Psi m$ function that in turn would trigger apoptosis signalling through mitochondrial pathway, ultimately leading to cell death by both the proteolytic cascade of pro-apoptotic enzymes and the damage caused to the mitochondrial function. These results should be considered when designing new hybrid materials for food-industry applications.

Acknowledgements

The authors gratefully acknowledge the financial support from the Spanish government (Project RTI2018-101599-B-C21 (MCUI/AEI/FEDER, EU)).

References

Abbasi, F., Hashemi, H., Samaei, M.R., SavarDashtaki, A., Azhdarpoor, A., Fallahi, M.J., 2021. The synergistic interference effect of silica nanoparticles concentration and the wavelength of ELISA on the colorimetric assay of cell toxicity. Sci. Rep. 11,

15133. https://doi.org/10.1038/s41598-021-92419-1

Abbaszadeh, S., Sharifzadeh, A., Shokri, H., Khosravi, A.R., Abbaszadeh, A., 2014. Antifungal efficacy of thymol, carvacrol, eugenol and menthol as alternative agents to control the growth of food-relevant fungi. J. Mycol. Med. 24, 51–56. https://doi.org/10.1016/J.MYCMED.2014.01.063

Abdelhamid, A.G., Yousef, A.E., 2021. Natural Antimicrobials Suitable for Combating Desiccation-Resistant Salmonella enterica in Milk Powder. Microorg. 2021, Vol. 9, Page 421 9, 421. https://doi.org/10.3390/MICROORGANISMS9020421

Aburawi, E.H., Qureshi, M.A., Oz, D., Jayaprakash, P., Tariq, S., Hameed, R.S., Das, S., Goswami, A., Biradar, A. V., Asefa, T., Souid, A.-K., Adeghate, E., Howarth, F.C., 2012. Biocompatibility of Calcined Mesoporous Silica Particles with Ventricular Myocyte Structure and Function. Chem. Res. Toxicol. 26, 26–36. https://doi.org/10.1021/TX300255U

Al-Salam, S., Balhaj, G., Al-Hammadi, S., Sudhadevi, M., Tariq, S., Biradar, A. V., Asefa, T., Souid, A.-K., 2011. In Vitro Study and Biocompatibility of Calcined Mesoporous Silica Microparticles in Mouse Lung. Toxicol. Sci. 122, 86–99. https://doi.org/10.1093/TOXSCI/KFR078

Alothman, Z., 2012. A Review: Fundamental Aspects of Silicate Mesoporous Materials. Materials (Basel). 5, 2874–2902. https://doi.org/10.3390/ma5122874

Aranda, A., Sequedo, L., Tolosa, L., Quintas, G., Burello, E., Castell, J. V., Gombau, L., 2013. Dichloro-dihydro-fluorescein diacetate (DCFH-DA) assay: A quantitative method for oxidative stress assessment of nanoparticle-treated cells. Toxicol. Vitr. 27, 954–963. https://doi.org/10.1016/j.tiv.2013.01.016

765 Aslantürk, Ö.S., 2018. In Vitro Cytotoxicity and Cell Viability Assays: Principles,
766 Advantages, and Disadvantages, in: Genotoxicity - A Predictable Risk to Our Actual
767 World. InTech. https://doi.org/10.5772/intechopen.71923

768 Bagheri, E., Ansari, L., Abnous, K., Taghdisi, S.M., Charbgoo, F., Ramezani, M.,
769 Alibolandi, M., 2018. Silica based hybrid materials for drug delivery and
770 bioimaging. J. Control. Release. https://doi.org/10.1016/j.jconrel.2018.03.014

771 Bakkali, F., Averbeck, S., Averbeck, D., Idaomar, M., 2008. Biological effects of
772 essential oils – A review. Food Chem. Toxicol. 46, 446–475.
773 https://doi.org/10.1016/j.fct.2007.09.106

774 Barrera, G., 2012. Oxidative Stress and Lipid Peroxidation Products in Cancer
775 Progression and Therapy. ISRN Oncol. 2012, 1–21.
776 https://doi.org/10.5402/2012/137289

777 Boelsterli, U.A., 2007. Mechanistic toxicology : the molecular basis of how chemicals
778 disrupt biological targets. CRC Press.

779 Burt, S., 2004. Essential oils: their antibacterial properties and potential applications in
780 foods—a review. Int. J. Food Microbiol. 94, 223–253.
781 https://doi.org/10.1016/J.IJFOODMICRO.2004.03.022

782 Čabarkapa, I., Čolović, R., Đuragić, O., Popović, S., Kokić, B., Milanov, D., Pezo, L.,
783 2019. Anti-biofilm activities of essential oils rich in carvacrol and thymol against
784 Salmonella Enteritidis. https://doi.org/10.1080/08927014.2019.1610169 35, 361–
785 375. https://doi.org/10.1080/08927014.2019.1610169

786 Cabrera, S., El Haskouri, J., Guillem, C., Latorre, J., Beltrán-Porter, A., Beltrán-Porter,
787 D., Marcos, M.D., Amorós, P., 2000. Generalised syntheses of ordered mesoporous

788 oxides: The atrane route. Solid State Sci. 2, 405–420. https://doi.org/10.1016/S1293-
789 2558(00)00152-7

790 Casey, A., Herzog, E., Lyng, F.M., Byrne, H.J., Chambers, G., Davoren, M., 2008. Single
791 walled carbon nanotubes induce indirect cytotoxicity by medium depletion in A549
792 lung cells. Toxicol. Lett. 179, 78–84.
793 https://doi.org/10.1016/J.TOXLET.2008.04.006

794 Chen, F., Shi, Z., Neoh, K.G., Kang, E.T., 2009. Antioxidant and antibacterial activities
795 of eugenol and carvacrol-grafted chitosan nanoparticles. Biotechnol. Bioeng. 104,
796 30–39. https://doi.org/10.1002/bit.22363

797 Ciappellano, S.G., Tedesco, E., Venturini, M., Benetti, F., 2016. In vitro toxicity
798 assessment of oral nanocarriers. Adv. Drug Deliv. Rev.
799 https://doi.org/10.1016/j.addr.2016.08.007

800 D'Arcy, M.S., 2019. Cell death: a review of the major forms of apoptosis, necrosis and
801 autophagy. Cell Biol. Int. 43, 582–592. https://doi.org/10.1002/CBIN.11137

802 Diab, R., Canilho, N., Pavel, I.A., Haffner, F.B., Girardon, M., Pasc, A., 2017. Silica-
803 based systems for oral delivery of drugs, macromolecules and cells. Adv. Colloid
804 Interface Sci. 249, 346–362. https://doi.org/10.1016/j.cis.2017.04.005

805 Eisenbrand, G., Pool-Zobel, B., Baker, V., Balls, M., Blaauboer, B.J., Boobis, A., Carere,
806 A., Kevekordes, S., Lhuguenot, J.C., Pieters, R., Kleiner, J., 2002. Methods of in
807 vitro toxicology. Food Chem. Toxicol. https://doi.org/10.1016/S0278-
808 6915(01)00118-1

809 Faleiro, M.L., Miguel, G., 2020. Antimicrobial and Antioxidant Activities of Natural
810 Compounds: Enhance the Safety and Quality of Food. Foods 2020, Vol. 9, Page

1145 9, 1145. https://doi.org/10.3390/FOODS9091145

Ferrer, E., Juan-García, A., Font, G., Ruiz, M.J., 2009. Reactive oxygen species induced by beauvericin, patulin and zearalenone in CHO-K1 cells. Toxicol. Vitr. 23, 1504–1509. https://doi.org/10.1016/j.tiv.2009.07.009

Fotakis, G., Timbrell, J.A., 2006. In vitro cytotoxicity assays: Comparison of LDH, neutral red, MTT and protein assay in hepatoma cell lines following exposure to cadmium chloride. Toxicol. Lett. 160, 171–177. https://doi.org/10.1016/J.TOXLET.2005.07.001

Fuentes, C., Ruiz-Rico, M., Fuentes, A., Barat, J.M., Ruiz, M.J., 2021. Comparative cytotoxic study of silica materials functionalised with essential oil components in HepG2 cells. Food Chem. Toxicol. 147, 111858. https://doi.org/10.1016/j.fct.2020.111858

Fuentes, C., Ruiz-Rico, M., Fuentes, A., Ruiz, M.J., Barat, J.M., 2020. Degradation of silica particles functionalised with essential oil components under simulated physiological conditions. J. Hazard. Mater. 399, 123120. https://doi.org/10.1016/j.jhazmat.2020.123120

García-Ríos, E., Ruiz-Rico, M., Guillamón, J.M., Pérez-Esteve, É., Barat, J.M., 2018. Improved antimicrobial activity of immobilised essential oil components against representative spoilage wine microorganisms. Food Control 94, 177–186. https://doi.org/10.1016/j.foodcont.2018.07.005

Garrido-Cano, I., Candela-Noguera, V., Herrera, G., Cejalvo, J.M., Lluch, A., Marcos, M.D., Sancenon, F., Eroles, P., Martínez-Máñez, R., 2021. Biocompatibility and internalization assessment of bare and functionalised mesoporous silica nanoparticles. Microporous Mesoporous Mater. 310, 110593.

https://doi.org/10.1016/J.MICROMESO.2020.110593

Hamilton, R.F., Thakur, S.A., Holian, A., 2008. Silica binding and toxicity in alveolar macrophages. Free Radic. Biol. Med. 44, 1246–1258. https://doi.org/10.1016/j.freeradbiomed.2007.12.027

Heikkilä, T., Santos, H.A., Kumar, N., Murzin, D.Y., Salonen, J., Laaksonen, T., Peltonen, L., Hirvonen, J., Lehto, V.-P., 2010. Cytotoxicity study of ordered mesoporous silica MCM-41 and SBA-15 microparticles on Caco-2 cells. Eur. J. Pharm. Biopharm. 74, 483–494. https://doi.org/10.1016/J.EJPB.2009.12.006

Herzog, E., Byrne, H.J., Davoren, M., Casey, A., Duschl, A., Oostingh, G.J., 2009. Dispersion medium modulates oxidative stress response of human lung epithelial cells upon exposure to carbon nanomaterial samples. Toxicol. Appl. Pharmacol. 236, 276–281. https://doi.org/10.1016/J.TAAP.2009.02.007

Holder, A.L., Goth-Goldstein, R., Lucas, D., Koshland, C.P., 2012. Particle-Induced Artifacts in the MTT and LDH Viability Assays. https://doi.org/10.1021/tx3001708

Hyldgaard, M., Mygind, T., Meyer, R.L., 2012. Essential oils in food preservation: Mode of action, synergies, and interactions with food matrix components. Front. Microbiol. 3, 1–12. https://doi.org/10.3389/fmicb.2012.00012

Jeong, S.Y., Seol, D.W., 2008. The role of mitochondria in apoptosis. J. Biochem. Mol. Biol. https://doi.org/10.5483/bmbrep.2008.41.1.011

Karam, L., Roustom, R., Abiad, M.G., El-Obeid, T., Savvaidis, I.N., 2019. Combined effects of thymol, carvacrol and packaging on the shelf-life of marinated chicken. Int. J. Food Microbiol. 291, 42–47. https://doi.org/10.1016/J.IJFOODMICRO.2018.11.008

858 Korhonen, E., Rönkkö, S., Hillebrand, S., Riikonen, J., Xu, W., Järvinen, K., Lehto, V.P.,
859 Kauppinen, A., 2016. Cytotoxicity assessment of porous silicon microparticles for
860 ocular drug delivery. Eur. J. Pharm. Biopharm. 100, 1–8.
861 https://doi.org/10.1016/J.EJPB.2015.11.020

862 Kroll, A., Pillukat, M.H., Hahn, D., Schnekenburger, J., 2012. Interference of engineered
863 nanoparticles with in vitro toxicity assays. Arch. Toxicol. 86, 1123–1136.
864 https://doi.org/10.1007/s00204-012-0837-z

865 Kyriakidou, K., Brasinika, D., Trompeta, A.F.A., Bergamaschi, E., Karoussis, I.K.,
866 Charitidis, C.A., 2020. In vitro cytotoxicity assessment of pristine and carboxyl-
867 functionalized MWCNTs. Food Chem. Toxicol. 141, 111374.
868 https://doi.org/10.1016/j.fct.2020.111374

869 Laaksonen, T., Santos, H., Vihola, H., Salonen, J., Riikonen, J., Heikkilä, T., Peltonen,
870 L., Kumar, N., Murzin, D.Y., Lehto, V.P., Hirvonen, J., 2007. Failure of MTT as a
871 toxicity testing agent for mesoporous silicon microparticles. Chem. Res. Toxicol.
872 20, 1913–1918. https://doi.org/10.1021/tx700326b

873 Lehman, S.E., Morris, A.S., Mueller, P.S., Salem, A.K., Grassian, V.H., Larsen, S.C.,
874 2016. Silica nanoparticle-generated ROS as a predictor of cellular toxicity:
875 Mechanistic insights and safety by design. Environ. Sci. Nano 3, 56–66.
876 https://doi.org/10.1039/c5en00179j

877 Meynen, V., Cool, P., Vansant, E.F., 2009. Verified syntheses of mesoporous materials.
878 Microporous Mesoporous Mater. 125, 170–223.
879 https://doi.org/10.1016/J.MICROMESO.2009.03.046

880 Miret, S., De Groene, E.M., Klaffke, W., 2006. Comparison of in vitro assays of cellular
881 toxicity in the human hepatic cell line HepG2. J. Biomol. Screen. 11, 184–193.

https://doi.org/10.1177/1087057105283787

Peña-Gómez, N., Ruiz-Rico, M., Fernández-Segovia, I., Barat, J.M., 2019a. Study of apple juice preservation by filtration through silica microparticles functionalised with essential oil components. Food Control 106, 106749. https://doi.org/10.1016/j.foodcont.2019.106749

Peña-Gómez, N., Ruiz-Rico, M., Pérez-Esteve, É., Fernández-Segovia, I., Barat, J.M., 2020. Microbial stabilization of craft beer by filtration through silica supports functionalized with essential oil components. LWT 117, 108626. https://doi.org/10.1016/j.lwt.2019.108626

Peña-Gómez, N., Ruiz-Rico, M., Pérez-Esteve, É., Fernández-Segovia, I., Barat, J.M., 2019b. Novel antimicrobial filtering materials based on carvacrol, eugenol, thymol and vanillin immobilized on silica microparticles for water treatment. Innov. Food Sci. Emerg. Technol. 58, 102228. https://doi.org/10.1016/j.ifset.2019.102228

Puerari, R.C., Ferrari, E., de Cezar, M.G., Gonçalves, R.A., Simioni, C., Ouriques, L.C., Vicentini, D.S., Matias, W.G., 2019. Investigation of toxicological effects of amorphous silica nanostructures with amine-functionalized surfaces on Vero cells. Chemosphere 214, 679–687. https://doi.org/10.1016/j.chemosphere.2018.09.165

Ray, P.D., Huang, B.-W., Tsuji, Y., 2012. Reactive oxygen species (ROS) homeostasis and redox regulation in cellular signaling. Cell. Signal. 24, 981. https://doi.org/10.1016/J.CELLSIG.2012.01.008

Ribes, S., Fuentes, A., Talens, P., Barat, J.M., 2018. Prevention of fungal spoilage in food products using natural compounds: A review. Crit. Rev. Food Sci. Nutr. 58, 2002–2016. https://doi.org/10.1080/10408398.2017.1295017

905 Ribes, S., Ruiz-Rico, M., Pérez-Esteve, É., Fuentes, A., Barat, J.M., 2019. Enhancing the
906 antimicrobial activity of eugenol, carvacrol and vanillin immobilised on silica
907 supports against Escherichia coli or Zygosaccharomyces rouxii in fruit juices by
908 their binary combinations. LWT 113, 108326.
909 https://doi.org/10.1016/j.lwt.2019.108326

910 Ribes, S., Ruiz-Rico, M., Pérez-Esteve, É., Fuentes, A., Talens, P., Martínez-Máñez, R.,
911 Barat, J.M., 2017. Eugenol and thymol immobilised on mesoporous silica-based
912 material as an innovative antifungal system: Application in strawberry jam. Food
913 Control 81, 181–188. https://doi.org/10.1016/J.FOODCONT.2017.06.006

914 Ros-Lis, J. V., Bernardos, A., Pérez, É., Barat, J.M., Martínez-Máñez, R., 2018.
915 Functionalized Silica Nanomaterials as a New Tool for New Industrial Applications,
916 in: Impact of Nanoscience in the Food Industry. Elsevier Inc., pp. 165–196.
917 https://doi.org/10.1016/B978-0-12-811441-4.00007-8

918 Ruiz-Leal, M., George, S., 2004. An in vitro procedure for evaluation of early stage
919 oxidative stress in an established fish cell line applied to investigation of PHAH and
920 pesticide toxicity. Mar. Environ. Res. 58, 631–635.
921 https://doi.org/10.1016/J.MARENVRES.2004.03.054

922 Saei, A.A., Yazdani, M., Lohse, S.E., Bakhtiary, Z., Serpooshan, V., Ghavami, M.,
923 Asadian, M., Mashaghi, S., Dreaden, E.C., Mashaghi, A., Mahmoudi, M., 2017.
924 Nanoparticle Surface Functionality Dictates Cellular and Systemic Toxicity. Chem.
925 Mater. 29, 6578–6595. https://doi.org/10.1021/ACS.CHEMMATER.7B01979

926 Samri, M.T. Al, Biradar, A. V, Alsuwaidi, A.R., Balhaj, G., Al-Hammadi, S., Shehab, S.,
927 Al-Salam, S., Tariq, S., Pramathan, T., Benedict, S., Asefa, T., Souid, A.-K., 2012.
928 In vitro biocompatibility of calcined mesoporous silica particles and fetal blood

cells. Int. J. Nanomedicine 7, 3111. https://doi.org/10.2147/IJN.S32711

Santos, H.A., Riikonen, J., Salonen, J., Mäkilä, E., Heikkilä, T., Laaksonen, T., Peltonen, L., Lehto, V.-P., Hirvonen, J., 2010. In vitro cytotoxicity of porous silicon microparticles: Effect of the particle concentration, surface chemistry and size. Acta Biomater. 6, 2721–2731. https://doi.org/10.1016/J.ACTBIO.2009.12.043

Severin, I., Souton, E., Dahbi, L., Chagnon, M.C., 2017. Use of bioassays to assess hazard of food contact material extracts: State of the art. Food Chem. Toxicol. 105, 429–447. https://doi.org/10.1016/J.FCT.2017.04.046

Shamsi, M. Al, Samri, M.T. Al, Al-Salam, S., Conca, W., Shaban, S., Benedict, S., Tariq, S., Biradar, A. V., Penefsky, H.S., Asefa, T., Souid, A.-K., 2010. Biocompatibility of Calcined Mesoporous Silica Particles with Cellular Bioenergetics in Murine Tissues. Chem. Res. Toxicol. 23, 1796–1805. https://doi.org/10.1021/TX100245J

Tait, S.W.G., Green, D.R., 2013. Mitochondrial regulation of cell death. Cold Spring Harb. Perspect. Biol. 5, a008706. https://doi.org/10.1101/cshperspect.a008706

Tippayatum, P., Chonhenchob, V., 2007. Antibacterial activities of thymol, eugenol and nisin against some food spoilage bacteria. Nat. Sci. 41, 319–23.

Vicentini, D.S., Puerari, R.C., Oliveira, K.G., Arl, M., Melegari, S.P., Matias, W.G., 2017. Toxicological impact of morphology and surface functionalization of amorphous SiO2 nanomaterials. NanoImpact 5, 6–12. https://doi.org/10.1016/J.IMPACT.2016.11.003

Walczak, M., Michalska-Sionkowska, M., Olkiewicz, D., Tarnawska, P., Warżyńska, O., 2021. Potential of Carvacrol and Thymol in Reducing Biofilm Formation on Technical Surfaces. Mol. 2021, Vol. 26, Page 2723 26, 2723.

https://doi.org/10.3390/MOLECULES26092723

Wang, C., Youle, R.J., 2009. The Role of Mitochondria in Apoptosis. Annu. Rev. Genet. 43, 95. https://doi.org/10.1146/ANNUREV-GENET-102108-134850

Weyermann, J., Lochmann, D., Zimmer, A., 2005. A practical note on the use of cytotoxicity assays. Int. J. Pharm. 288, 369–376. https://doi.org/10.1016/J.IJPHARM.2004.09.018

Xu, J., Zhou, F., Ji, B.P., Pei, R.S., Xu, N., 2008. The antibacterial mechanism of carvacrol and thymol against Escherichia coli. Lett. Appl. Microbiol. 47, 174–179. https://doi.org/10.1111/j.1472-765X.2008.02407.x

Xu, J.J., Diaz, D., O'Brien, P.J., 2004. Applications of cytotoxicity assays and pre-lethal mechanistic assays for assessment of human hepatotoxicity potential. Chem. Biol. Interact. 150, 115–128. https://doi.org/10.1016/J.CBI.2004.09.011

Zhang, Y., 2018. Cell toxicity mechanism and biomarker. Clin. Transl. Med. 7, 34. https://doi.org/10.1186/s40169-018-0212-7